

Development and Application of an Efficient FDTD / Haar MRTD Numerical Interface

Costas D. Sarris and Linda P. B. Katehi

Radiation Laboratory, Department of Electrical Engineering and Computer Science
University of Michigan, Ann Arbor, 48109-2122, MI

Abstract-A numerically stable interface between the Haar wavelet based MRTD technique and FDTD is presented in this paper. Such a hybridization of MRTD facilitates the application of the method to open structures and inhomogeneous circuit geometries, where the use of high order wavelets significantly complicates the formulation of a pure MRTD scheme. Furthermore, it allows for the straightforward enforcement of localized boundary conditions, bypassing the necessity to employ image theory, which typically arises in MRTD. The fact that the implementation of the proposed interface involves no spatial or temporal interpolation indicates the efficiency of the developed technique.

Keywords-Multiresolution Analysis, MRTD, FDTD.

I. INTRODUCTION

The time domain characterization of microwave structures, often encountered in wireless front-end applications such as filter, resonator or feed components, usually includes the modeling of fine detail complex boundaries and regions of dynamically varying field distributions [1]. Therefore, the incorporation of mesh refinement techniques, that offer the promise of alleviating the computational burden, brought about by the stability restriction that the necessarily fine cell size imposes on the time step, is motivated.

Standard subgridding techniques involve spatio-temporal interpolations or extrapolations at the boundaries of different resolution parts of the numerical grid [2], that render the rigorous enforcement of the divergence free nature of the magnetic field and the continuity conditions a rather subtle issue. Furthermore, a higher order static subgridding algorithm for the Finite Difference Time Domain (FDTD) technique, that needs no interpolatory operations was recently proposed [3]. However, as time domain simulations of microwave geometries typically register the history of a wideband pulse propagation along the computational domain, adaptively imposing dense gridding conditions only in and around the pulse and the products of its retro-reflections can further extend the efficiency of a technique. Thus, if allowing for a relatively coarse mesh is one challenge that novel numerical schemes are expected to meet, a second, but equally important one, is adaptivity, translating to the possibility of dynamic mesh refinement at regions of the domain that are electromagnetically active at a certain time step.

Wavelet based numerical algorithms stemming from the Multiresolution Time Domain technique [4] offer a natural framework for the implementation of dynamic mesh refinement as shown in [5]. For homogeneous domains, the computational efficiency of the former, is expected to increase with the order of the multiresolution expansion at hand [6]. Yet, the complexity of conductor, dielectric and boundary modeling that they present,

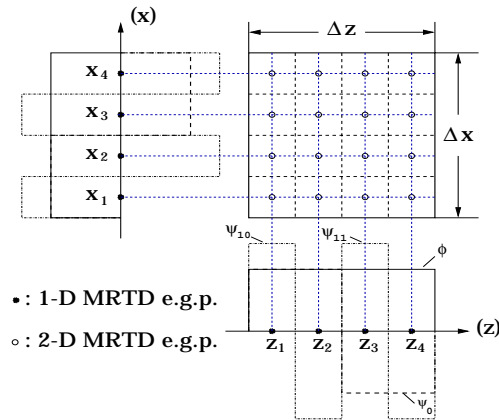


Fig. 1. Equivalent grid points (e.g.p.) within a scaling cell as introduced by a first order wavelet expansion in x, z directions.

also increasing with wavelet order, seriously compromises their potential applicability to state of the art devices. The aforementioned contradiction is addressed in this paper by means of a hybrid approach that connects the FDTD technique with the Haar wavelet based MRTD, via a numerical interface. The purpose of this approach is to establish an efficient algorithm, allowing for the combination of the versatility of FDTD with the adaptivity of MRTD, employing the first in geometrically complex parts of the domain and the second in homogeneous regions.

II. FORMULATION

A. MRTD, FDTD equations

A two dimensional system of the following Maxwell's equations, corresponding to TE waves :

$$\frac{\partial E_y}{\partial t}(\bar{p}, t) = \frac{1}{\epsilon} \left(\frac{\partial H_x}{\partial z}(\bar{p}, t) - \frac{\partial H_z}{\partial x}(\bar{p}, t) \right) \quad (1)$$

$$\frac{\partial H_x}{\partial t}(\bar{p}, t) = \frac{1}{\mu} \frac{\partial E_y}{\partial z}(\bar{p}, t) \quad (2)$$

$$\frac{\partial H_z}{\partial t}(\bar{p}, t) = -\frac{1}{\mu} \frac{\partial E_y}{\partial x}(\bar{p}, t) \quad (3)$$

with $\bar{p} = x\hat{x} + z\hat{z}$, is considered and discretized following the Moment Method based technique of [4]. In the MRTD region, the field components are expanded in a Haar wavelet basis of orders $r_{x,max}$ in x - and $r_{z,max}$ in z - direction respectively, the scaling cell sizes being denoted by Δx , Δz . As explained in [7], if an electric field scaling cell is centered at $(i\Delta x, k\Delta z)$, the corresponding H_x scaling cell must be centered at $(i\Delta x, (k + s_z)\Delta z)$, with $s_z = 1/2^{r_{z,max}+2}$, while the H_z one at $((i + s_x)\Delta x, k\Delta z)$, with $s_x = 1/2^{r_{x,max}+2}$. In the

FDTD region, the field components are expanded in a pulse basis, introducing the cell dimensions $\Delta\xi_{eff} = \Delta\xi/2^{r_{\xi,max}+1}$, $\xi = x, z$. For example, the H_x expansion in the MRTD region is cast in the form :

$$\begin{aligned} H_x(\bar{p}, t) = & \sum_{n,i,k} h_{n+\frac{1}{2}}(t) \left\{ \begin{aligned} & H_{i,k+s_z}^{x,\phi\phi} \phi_i(x) \phi_{k+s_z}(z) \\ & + \sum_{r_x,p_x} H_{i,k+s_z}^{x,\psi_{r_x,p_x}\phi} \psi_i^{r_x,p_x}(x) \phi_{k+s_z}(z) \\ & + \sum_{r_z,p_z} H_{i,k+s_z}^{x,\phi\psi_{r_z,p_z}} \phi_i(x) \psi_{k+s_z}^{r_z,p_z}(z) \\ & + \sum_{r_x,p_x,r_z,p_z} H_{i,k+s_z}^{x,\psi^{r_x,p_x}\psi_{r_z,p_z}} \psi_i^{r_x,p_x}(x) \psi_{k+s_z}^{r_z,p_z}(z) \end{aligned} \right\} \end{aligned}$$

where the standard definitions (given for example in [8]) have been used for the Haar scaling and wavelet functions $\phi, \psi^{r,p}$ and the pulse functions h (which compose the temporal basis of the method). In the FDTD region, $H_x(\bar{p}, t)$ is written as :

$$H_x(\bar{p}, t) = \sum_{n,i,k} h_{n+\frac{1}{2}}(t) \left\{ H_{i,k+1/2} \phi_i^{r_{x,max}+1}(x) \phi_{k+\frac{1}{2}}^{r_{z,max}+1}(z) \right\}$$

where the definition of the r -order scaling function : $\phi_m^r(\xi) = 2^{r/2} \phi(2^r(\xi/\Delta\xi) - m)$ with $\xi = x, z$ has been adopted. The use of Haar wavelets in the MRTD region, effectively divides each scaling cell into $2^{r_{x,max}+1} \times 2^{r_{z,max}+1}$ subcells of size Δx_{eff} by Δz_{eff} , in the sense shown in Fig. 1, where the case of a first order (two wavelet levels) in both x, z directions scheme is depicted. An MRTD dispersion analysis [9] leads to the following expression :

$$\left\{ \frac{1}{u_p \Delta t} \sin \frac{\omega \Delta t}{2} \right\}^2 = \left\{ \frac{1}{\Delta x_{eff}} \sin \frac{k_x \Delta x_{eff}}{2} \right\}^2 + \left\{ \frac{1}{\Delta z_{eff}} \sin \frac{k_z \Delta z_{eff}}{2} \right\}^2 \quad (4)$$

which coincides with the dispersion relationship of an FDTD scheme with cell sizes $\Delta x_{eff}, \Delta z_{eff}$, as the one considered here (u_p denotes the phase velocity). Hence, under the electric / magnetic node arrangement that is used for the MRTD region, a perfect matching of the stability and dispersion properties of the methods applied in the two regions is attained, leading to their reflectionless and stable connection with no need for any interpolation or extrapolation in either space or time.

B. Connection Algorithm

Expanding on the concepts presented in [8], a two dimensional connection algorithm is developed. Considering the case where an FDTD region encloses an MRTD one, the data transfer from MRTD to FDTD is initially addressed. It is noted that for the update of all FDTD grid points whose stencil extends into the MRTD region, it suffices to retrieve the nodal field values of the electric field one FDTD cell within the MRTD region (Fig. 2), thus allowing for the complete determination of the tangential electromagnetic field components across the boundary of the FDTD domain. Then, by equivalence principle, the independent solution of this region becomes possible. Thus, the problem

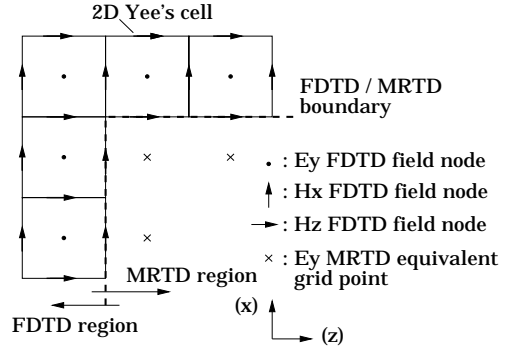


Fig. 2. FDTD update from MRTD data.

boils down to calculating nodal field values across the boundary of the MRTD region, which is exactly the inverse fast wavelet transform (IFWT) function that is carried out at the optimal complexity of $\mathcal{O}(N)$. Conversely, for the update of the MRTD boundary magnetic field coefficients, FDTD electric field nodes extending over one scaling cell within the FDTD region are wavelet transformed, via a fast wavelet transform (FWT) routine. If this scaling cell extends beyond the domain, zero field values are used. This is possible for both closed and open domain problems, since a PEC backed absorber is normally used for the simulation of an open boundary. Fig. 3 schematically explains this procedure, for a case where $r_{x,max} = r_{z,max} = 1$. It is noted that no FDTD grid points are sought at the (shaded) corner region shown in Fig. 3. This is due to the fact that MRTD, just as FDTD, uses a cross - shaped stencil for the update of all grid points. Computing the electric field MRTD coefficients from the FDTD data via an FWT and updating the tangential magnetic field component coefficients via the standard MRTD finite difference equations, determines again the tangential electromagnetic field components across the boundary of the MRTD region, which is sufficient for its independent, MRTD based solution.

Evidently, all operations that implement this connection algorithm are performed at the same time step, during the update of the electric field coefficients in both regions, in an absolutely stable fashion, due to the matching of the dispersion properties of the two schemes. Furthermore, the same principles lead to interfaces between wavelet schemes of an arbitrary basis and the ones that are formulated by the corresponding scaling functions only, provided that the effective resolutions in the two regions are kept the same. It is also noted that the extension of the interface algorithm to three dimensions is accomplished by treating each face of Yee's cell according to the method that has been set forth in this work.

III. NUMERICAL RESULTS

A. Validation

A simple two dimensional air filled square resonator (shown in Fig. 4) is analyzed for validation purposes. The dimensions are normalized and given in terms of equivalent FDTD grid points. The MRTD region is only two grid points away from the PEC walls of the resonator. A pure MRTD scheme would model these walls by means of image theory, necessitating the

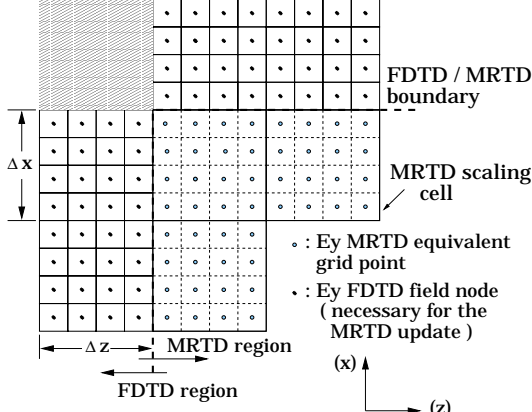


Fig. 3. MRTD update from FDTD data.

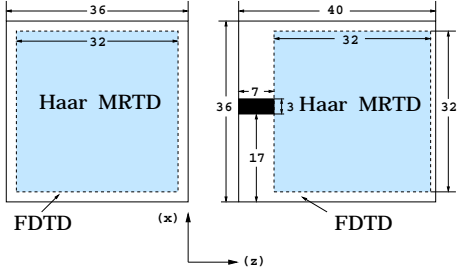


Fig. 4. Empty square cavity geometry, metal finned loaded cavity and mesh (dimensions are given in FDTD grid points).

introduction of several images for a high wavelet order. However, in this study, enclosing the MRTD region in an FDTD one, facilitates the treatment of these hard boundaries, whose FDTD modeling amounts to setting the tangential to PEC electric field nodal values equal to zero. The patterns of the TE_{21} and TE_{22} - modes derived via the interface algorithm for MRTD schemes with $r_{x,max} = r_{z,max} = 4$ (1 by 1 scaling cell) and $r_{x,max} = 2$, $r_{z,max} = 3$ (4 by 2 scaling cells) respectively, are shown in Figures 5, 6. In both cases, a time step equal to 0.9 of the stability limit was used. In addition, TE_{22} is determined by a zero by zero order MRTD scheme (16 by 16 scaling cells) applied in the MRTD region of the domain, keeping the same number of degrees of freedom as before. The terms of the multiresolution expansion are then plotted in Fig. 7, to verify that their wavelet constituents assume the form of the spatial derivatives of the field, while a coarsely resolved field pattern is represented by scaling coefficients. Each plot is normalized with respect to the maximum and presented in a -25 to 0 logarithmic scale.

B. Application : Metal Fin Loaded Cavity

The method of this paper is tested in a metal fin loaded cavity, similar to the one presented in [10]. This structure is chosen for the reason that the presence of the metal fin within the domain, restricts the order of the MRTD scheme that can be employed for its analysis. In particular, whenever a scaling cell greater than the fin dimensions is chosen, utmost care is necessary for the compensation of the unphysical coupling of the regions below and above the fin, caused by the scaling function defining the fin cell (or wavelets extending beyond the fin limits). However, the strategies that are followed in this case (for example domain split), result in a local increase of operations and consumption of computational resources.

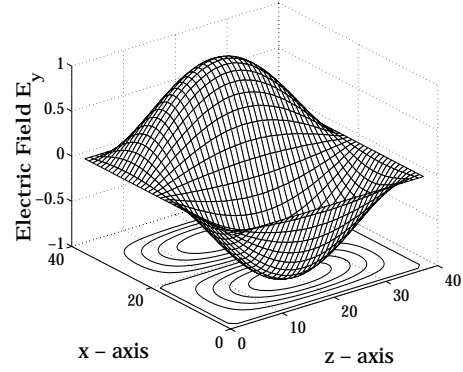


Fig. 5. Electric field pattern for the TE_{21} - mode of the empty cavity of Fig. 4 (4 by 4 MRTD).

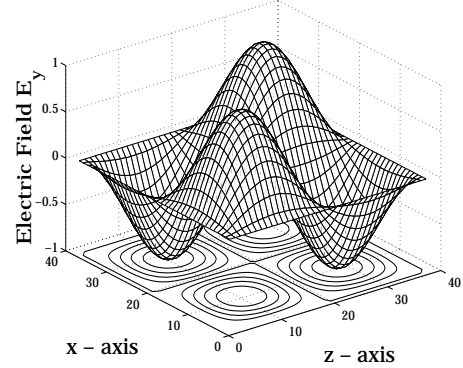


Fig. 6. Electric field pattern for the TE_{22} - mode of the empty cavity of Fig. 4 (2 by 3 MRTD).

For the interface based solution of the problem, the gridding conditions are given in Fig. 4. In the MRTD region, a second by second order scheme is employed (4 by 4 scaling cells). The time step is set at 0.8 of the Courant limit and FDTD cells of 1 cm by 1 cm are used. As an excitation, a Gaussian pulse, with its 3-dB frequency chosen to be equal to $f_c/2$, f_c being the cut-off frequency of the TE_{11} mode of the cavity, is applied in the FDTD region (at the plane $z = 5$ cm). Under these conditions, an absolutely stable performance of the code was observed. The deduced electric field spatial distribution is shown in Fig. 8. Moreover, in order to demonstrate the stability of the solution, the electric field, sampled at the point ($x = 1.55$ cm, $z = 2.35$ cm), is plotted as a function of time for an arbitrary interval of 18,000 - 20,000 time steps, in Fig. 9.

C. Application : Fractional cell PML termination

Utilizing the concept of the FDTD / MRTD interface, a Perfectly Matched Layer (PML) termination of the MRTD domain extending over a fraction of the MRTD scaling cell can be implemented. FDTD grid points beyond the conductor that backs the PML are simply zeroed out. Using this method, the waveguide structure of Fig. 10 is solved, by a fourth order MRTD scheme, truncated with a 6 and 8 grid point PML corresponding to 0.1875 and 0.25 of a scaling cell, which in this case is 8 mm. A 0 - 30 GHz Gaussian pulse excitation is used, and the reflection coefficient is calculated. Fig. 11 depicts comparative plots of the numerical results derived by the two termination types, along with the theoretical S_{11} form derived by transmission line

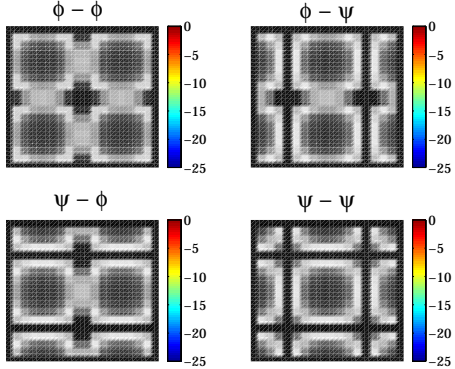


Fig. 7. Multiresolution constituent terms ($\phi - \phi$, $\phi - \psi$, $\psi - \phi$, $\psi - \psi$) of the TE_{22} mode pattern, determined by 0 by 0 order MRTD.

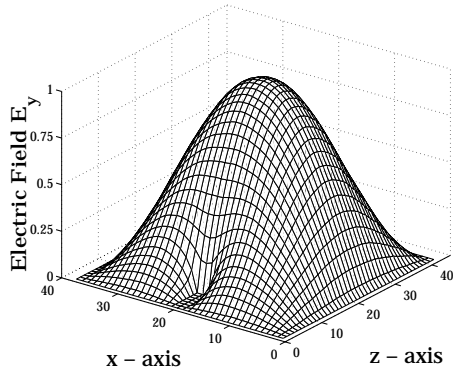


Fig. 8. Electric field distribution for the metal fin loaded cavity.

theory, demonstrating the excellent agreement of the two.

IV. CONCLUSIONS

A numerical interface between an arbitrary order Haar MRTD and FDTD was developed and applied in this paper. The two unique features of the proposed technique are that first, it does not employ any interpolations or extrapolations and second, it is applicable for *any* MRTD order. Hence, the developed algorithm constitutes a computationally efficient tool for jointly exploiting the advantages of FDTD and MRTD, which is critical for the acceleration of time domain schemes, when applied to large scale problems of current microwave technology applications.

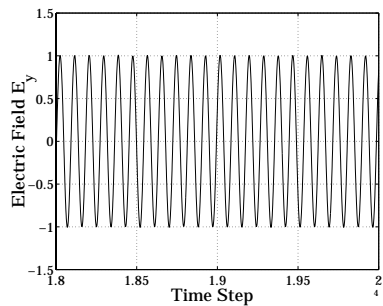


Fig. 9. Electric field sampled within the fin loaded cavity as a function of time for time steps 18,000-20,000.

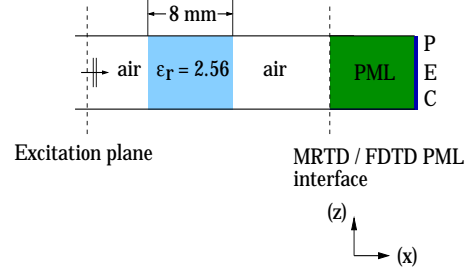


Fig. 10. Slab waveguide geometry.

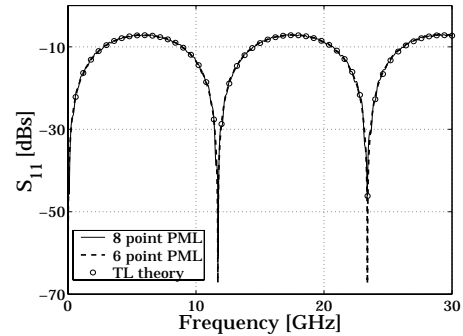


Fig. 11. Numerical and theoretical S_{11} for the slab geometry.

V. ACKNOWLEDGEMENTS

The authors acknowledge an illuminating communication with Professor W. J. R. Hoefer and Dr. M. Fujii on the motivation and performance of their TLM / Haar MRTD numerical interface.

This research has been supported by the Army Research Office under the project for “Efficient Numerical Solutions to Large Scale Tactical Communication Problems” (DAAD19-00-1-0173).

REFERENCES

- [1] R. Lotz, F. Arndt, “Advanced subgrid FD technique for modeling waveguide structures with curved conducting and dielectric boundaries”, *Proceedings of the 30th European Microwave Conference*, pp. 288-291, Paris, France, October 2000.
- [2] I. S. Kim, W. J. R. Hoefer, “A Local Mesh Refinement Algorithm for the Time Domain Finite Difference Method Using Maxwell’s Curl Equations”, *IEEE Trans. Microwave Theory Tech., MTT-38*, no.6, June 1990, pp. 812-815.
- [3] J. Ritter, F. Arndt, “A generalized 3D subgrid technique for the FDTD method”, *1997 IEEE MTT-S International Microwave Symposium Digest*, pp. 1563 - 1566.
- [4] M. Krumpholz, L.P.B. Katehi, “MRTD: New Time Domain Schemes Based on Multiresolution Analysis”, *IEEE Trans. Microwave Theory and Techniques*, vol.44, no.4, pp.555-561, April 1996.
- [5] E. Tentzeris, R. Robertson, A. Cangellaris and L.P.B. Katehi, “Space- and Time- Adaptive Gridding Using MRTD”, *1997 IEEE MTT-S International Microwave Symposium Digest*, pp.337-340.
- [6] M. Walter, I. Wolff, “An Algorithm for Realizing Yee’s FDTD method in the Wavelet Domain”, *1999 IEEE MTT-S International Microwave Symposium Digest*, pp. 1301-1304.
- [7] C. D. Sarris, L. P. B. Katehi, “Fundamental Gridding Related Dispersion Effects in MRTD schemes”, *2001 IEEE MTT-S International Microwave Symposium*, submitted.
- [8] C. D. Sarris, L. P. B. Katehi, “On the use of wavelets for the implementation of high order mesh refinement in time domain simulations”, *Proceedings of the 30th European Microwave Conference*, pp. 284-287, Paris, France, October 2000.
- [9] C. D. Sarris, L. P. B. Katehi, “Some Aspects of Dispersion Analysis of MRTD Schemes”, *2001 Review of Progress in Applied Computational Electromagnetics*, submitted.
- [10] M. Fujii, P.P.M. So, E. Hu, W. Liu, W. J. R. Hoefer, “A 2D TLM and Haar MRTD Real Time Hybrid Connection Algorithm”, *Proceedings of the 2000 ACES Conference*, pp. 1013-1020, Monterey, CA.